RSC Advances

PAPER

View Article Online
View Journal | View Issue

Cite this: *RSC Adv.*, 2022, **12**, 10178

Explicating the amino acid effects for methane storage in hydrate form

Sai Kiran Burla, [ab] S. R. Prasad Pinnelli *[ab] and Kalachand Sain[c]

Methane emissions increase day by day into the atmosphere and influence global temperatures. The necessity to capture these emissions at the source point is a primary concern. Several methods/techniques are being adopted to capture these emissions. The methane hydrates could be a viable method among them. The present study exposes various amino acids' effects in methane hydrate formation. The formation temperatures are around ~268 to 273 K except for l-cys, which is about ~277 K. The required subcooling for hydrates to trigger is high and is increasing in the order l-thr > l-met > l-phe > l-val > l-cys. The methane hydrate conversion is high in the presence of nearly all the amino acids with methane uptake capacity of ~80–85%, except l-thr, for which it is only 30% of the total uptake capacity. The side chain of l-thr comprises the hydroxyl group, making it a polar and uncharged amino acid. It is ascertained that hydroxyl groups alone can form hydrogen bonds with water, increasing the hydrophilicity and solubility of molecules, causing lesser conversion in the l-thr system. The gas uptake kinetics is faster in l-met and l-phe systems (t_{90} ~ 40 min), and sluggish kinetics is observed in l-cys, l-val, and l-thr systems. The investigations positively indicate using amino acids, l-met, l-phe, l-cys, and l-val as efficient materials for methane gas capture and storage in hydrate form, although not l-thr. Amino acids are readily dissolvable in water and could be easily pelletized for methane gas storage and transportation.

Received 25th January 2022
Accepted 22nd March 2022

DOI: 10.1039/d2ra00531j

rsc.li/rsc-advances

1 Introduction

1.1 Methane gas

Methane (CH_4) is an essential natural gas constituent and combustion gas. It is 25 times more potent than carbon dioxide (CO_2) for trapping heat. Anthropogenic methane emissions are increasing, and this influences global climate conditions. The source of emissions into the atmosphere are many, but the probable methods to capture and store the gas are limited.[1]

1.2 Natural gas hydrates

Ideally, clathrate hydrates combine "guest" and "host" molecules. In most scenarios, the gas molecules act as guests, and probably the water molecules as the host. The water molecules develop into cavities, and the gas molecules occupy these cages when favorable high pressure and low-temperature conditions prevail. The confinement of the guest molecules into the cages is due to weak van der Waal interactions. The hydrate structures are crystallized into sI, sII, and sH (s-structure) based on the guest molecule type.[2]

Natural gas hydrates are a vital energy reservoir with fuel gas.[3] These deposits occur naturally, and their presence is confirmed in marine sediments and permafrost regions at various locations on the earth. The gas constituent in these natural hydrates is mostly methane, and most reserves are untapped. It is specified that if 15% of these hydrate resources are exploited, it could fulfill the world's energy needs for more than 100 years at the current consumption rate.[4] Feasible technology to recover methane from the natural hydrates reserves is developing.[5,6] If feasibly exploited from the hydrate source, massive storage units/tanks are required to preserve and transport the gas. The gas pipeline networks could also not serve the purpose since most of the hydrate reserves are inaccessible to the pipeline network. It would be interesting if the recovered methane could be stored, preserved, and transported in synthetic hydrate form.[7–9]

1.3 Synthetic gas hydrates

Initially, the gas hydrate research started solely as scientific interest. It is observed that the hydrate form and create blockages in the pipeline network of the petroleum/gas industries. Further, research exertions are peaked to find a possible solution to mitigate this problem.[2] Hydrate blockages are controlled by thermodynamic (THIs), kinetic inhibitors (KHIs), and anti-

[a]*Gas Hydrate Division, CSIR-National Geophysical Research Institute (CSIR-NGRI), Hyderabad-500 007, India. E-mail: psrprasad@ngri.res.in; Fax: +91 40 2717 1564; Tel: +91 40 2701 2710*

[b]*Academy of Scientific and Innovative Research (AcSIR), Ghaziabad-201002, India*

[c]*Wadia Institute of Himalayan Geology (WIHG), 33 GMS Road, Dehradun-248001, Uttarakhand, India*

agglomerates. THIs move the hydrate phase boundary curve to the left, causing the requirement of low temperatures and high-pressure conditions. Glycols and alcohols act as THIs and permanently inhibit hydrate formation. The kinetic hydrate inhibitors are water-soluble polymers and delay hydrate formation.[10,11] The anti-agglomerates prevent the agglomeration of hydrate particulates, and the flow-related issues are minimized with small-sized hydrates.[12,13]

Further, the gas hydrates formation/constitution is striking, and many global research groups are pursuing their potential for various applications. Synthetic hydrates have been modules for specific gas selectivity and massive storage. Their high volumetric compression ability makes them more peculiar for gas storage applications.[14,15] This paved the way for many productive hydrate investigations for storage, separation, and transportation in the gas industry.[9,16–18] Besides, the hydrate methodology is helpful in the carbon dioxide capture and storage (CCS),[19,20] and also in desalination technology.[21]

The ideal gas intake capacity based on some model calculations (CSMGem)[3] for CH_4 hydrates is 170.4 v/v (ideal). It is challenging to populate all the cages, and the practical, achievable limit is 157.5 v/v. The perceptible drawbacks of employing hydrate technology for real-time gas storage and transportation applications are the slow process kinetics and ineffective hydrate conversion.[3] It is observed that a screen layer forms at the gas–water interface. It does not allow further gas to interact with water hindering hydrate growth.[22,23] Several mechanical techniques are being adopted to overcome these challenges and enhance the gas water interaction and higher surface area for hydrate growth.[24,25] These include mixing/agitating the sample using stirred reactor, rocking cells, and spraying the water into pressurized reactors using the high-pressure pumps.[26–28] Organic solvents and porous materials are also being studied to address these problems.[29–31] The search for novel material is still pursued to accelerate these processes for rapid kinetics and higher hydrate conversion. The research on diverse constituents, which do not participate in actual hydrate cage formation but accelerate the process, are being pursued rigorously.[30,32–34] Among these constituents, particles are the amino acids that could serve the need.[35]

1.4 Amino acids

Amino acids (AAs) are fine powders and are readily soluble in water. These powders are remarkable since they are readily soluble in water through hydrogen bonding and are biodegradable and non-toxic. These amino acids are available in twenty forms and are mainly seen in proteins. Depending on their side chair interaction with polar solvents, they are distinguished into hydrophobic and polar.[36] The structural properties and the hydrophobicity of selected amino acids powders are presented in Table 1. Amino acids are a class of organic compounds showing zwitterionic nature. They contain both amino and carboxylic groups. The isoelectric point (pI) severely depends on the side chain.[36] When tested to the methane hydrate process, some amino acids act as thermodynamic inhibitors.[37–43] This study objects to assess the CH_4 storage capacity in hydrate from using five different amino acid powders, primarily found in proteins, namely L-valine (l-val), L-phenylalanine (l-phe), L-cysteine (l-cys), L-methionine (l-met), and L-threonine (l-thr) under isochoric conditions. Methodical experiments are conducted in non-stirred configurations. Since stirring process could be huge and undesirable in real time practice, we examined the systems in a non-stirred condition,[44] Which could be quickly adopted for the real-time scale-up process. The length, side-chain type, and hydrophobicity factors are different for the selected amino acids.

2 Experimental method

2.1 Materials required for the hydrate formation

The sample powders of amino acid are obtained from M/S Sigma Aldrich and are used as received. The methane gas with purity (99.95%) is used for the experiments obtained from M/S Bhuruka Gas Company. The deionized millipore water type 1 is used in the sample preparation.

2.2 Apparatus and procedure followed to form the hydrate

The experiments were performed in a batch-type high-pressure reactor of volume 250 ml. The isochoric method is adopted for hydrate formation.[30,45,46] The experimental arrangement is presented in Fig. 1. The high-pressure reactor is cleaned thoroughly before the sample is loaded into the reactor. Extreme care is taken to avoid any contamination. The sample of volume 29 ml is loaded into the reactor chamber. The sample solution is prepared with deionized water and significantly less 0.5 wt% of the amino acid powder. Now the reactor head is mounted and sealed tightly using the screws. The experimental gas methane is pressurized into the reactor through inlet value using an ISCO syringe pump. Before pressurizing the reactor, the chamber is pressurized multiple times with the experimental gas to remove the atmospheric contaminants. The initial pressure is 5500 kPa@298 K. The chiller is set to increase or decrease the reactor temperature. Water and glycol mixture in aspect ratio is used as a coolant. The hydrate occurrence is indicated by an abrupt pressure reduction with a temperature spike resulting in the exothermic reaction. A platinum resistance thermometer (Pt100) measures the vessel's temperature. The pressure measurements are done with a WIKA pressure transducer (WIKA, type A-10 for pressure range 0–16 MPa). Uncertainties related with the temperature and pressure measurements are $\pm$0.5 K and 2%. The pressure and temperature readings are logged at specific intervals.

2.3. Equations used for calculating and inferring the data

The equation for calculating the amount of gas consumed during the hydrate formation. The content of gas (moles) in the hydrate phase during the experiment at time t is defined by the following equation:

$$\Delta nH, t \ = ng, 0 - ng, t = \left[\frac{P0V}{Z0RT0}\right] - \left[\frac{PtV}{ZtRTt}\right] \quad (1)$$

Table 1 The present study's structural and physical properties of amino acid powders

	Structure	Hydrophobicity[a]	Iso-electric point[a]	Solubility in water[b]
L-Valine	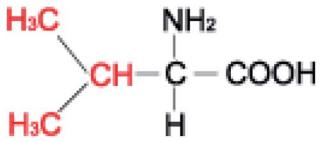	4.2	5.97	50 g L^{-1}
L-Phenylalanine	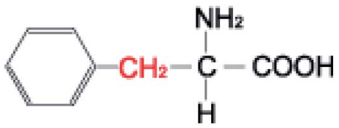	2.8	5.48	50 g L^{-1}[c]
L-Cysteine	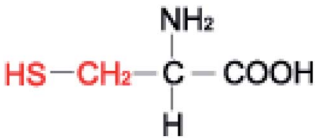	2.5	5.07	25 g L^{-1}
L-Methionine	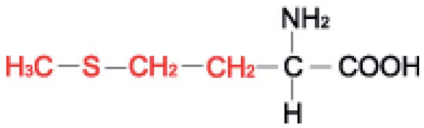	1.9	5.74	50 g L^{-1}[d]
L-Threonine	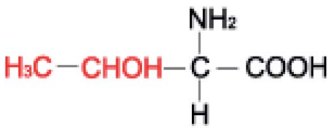	−0.7	5.87	50 g L^{-1}

[a] Data gathered from literature. [b] Data from Sigma Aldrich. [c] 1 M NH_4OH. [d] 1 M HCl.

The compressibility factor Z is calculated using the Peng–Robinson equation of state. P – pressure, V – volume, T – temperature, R – gas constant. 0 – initial point, t – a point at any given time.

The gas volume (V) was assumed constant during the experiments. The volume changes due to hydrate formation are neglected. $ng,0$ and ng,t denotes the number of moles of feed

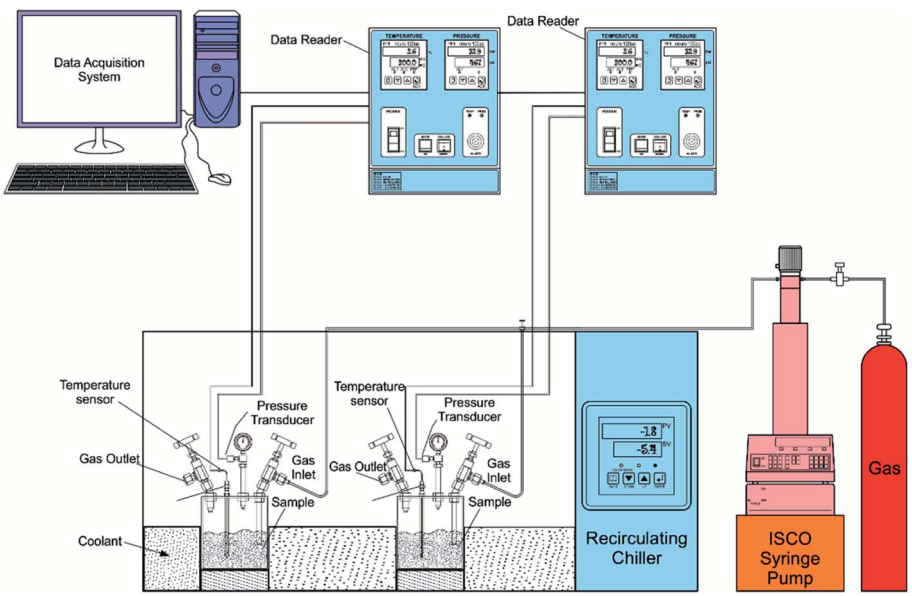

Fig. 1 Experimental setup used for the methane hydrate formation.

gas at hydrate nucleation point and in the gas phase at any time t, respectively.

The equation for calculating the gas uptake (v/v). The volumetric gas uptake (v/v) is calculated using the following equation.[47] It is defined as the "volume of gas/volume of water (hydrate + unreacted)."

$$v_t = \frac{\Delta n_t \times 22\,400}{(n_{H_2O} - 6.8\ \Delta n_t)\ \left(MW_{H_2O}/\rho_{H_2O}\right) + \left(\Delta n_t \times MW_{hydrate}/\rho_{hydrate}\right)} \quad (2)$$

where Δn_t is the mole of gas consumed, n_{H_2O} is the mole of water used, MW_{H_2O} is the molecular weight of water, ρ_{H_2O} is the density of water and $MW_{hydrate}$,$\rho_{hydrate}$ are the methane hydrate molecular weight and density calculated using the CSMGem application.[3]

3 Results and discussion

3.1 Methane hydrates formation and dissociation in the presence of amino acids

The amino acids are fine powders and readily soluble in water. 0.5 wt% is added to the sample solution and used as a reactant. Initially, the operating conditions are about 5500 kPa at 298 K. The amino acids used in this study are L-methionine (l-met), L-phenylalanine (l-phe), L-valine (l-val), L-cysteine (l-cys), and L-threonine (l-thr). The hydrate formation with pure water (without additive) is performed as a control experiment. Fig. 2 shows the pressure-temperature profiles of the methane hydrates formed in the presence of different amino acids.

In Fig. 2, the pressure-temperature profiles for the hydrates formed with l-met (a), l-phe (b), l-val (c), l-cys (d), and l-thr (e) are represented. The methane hydrate formation in pure water (without additive) at these operating conditions is shown in Fig. 2f. It is observed there is no hydrate formation in the pure water system. The linear decrement in the pressure is due to lowered temperature, and with an increase in temperature, the gas linearly retraces the cooling path. The black and red dots represent the hydrates' formation and dissociation pattern. The blue dashed line represents the phase boundary line of (sI) CH_4 hydrate generated using the CSMGem applications.[3] It is observed that the selected amino acids show an excellent affinity for the methane gas to form hydrates.

The chiller temperature is lowered, and the gas in the reactor tends to decrease linearly with a decrease in temperature. After crossing the phase boundary line, further decrement is observed in the pressure, and at a point, a sudden rise in temperature and diminution in pressure is seen. The point at an increase in temperature is considered a hydrate crystallization/nucleation point. The hydrate growth reaches saturation with additional process time and behaves linearly further as the temperature is lowered. The chiller is now set to higher temperatures to dissociate the hydrate. The red dots denote the hydrate dissociation and are directed and followed along the phase boundary line. The hydrate dissociation is done at 0.5–1 K h^{-1} (ideally, it could be completed at a quicker heating rate for degasifying). The deviation of the dissociation line at higher pressures is due to the faster heating rate.[48] The experiments are executed three times, and the average value is taken for demonstration. The pressure–temperature profiles of single-cycle are shown in the graph to avoid clumsiness. The formation temperatures range from ~268 to 273 K except for l-cys, about ~277 K. The pure water with no additive is performed as a control experiment. It does not show any significant hydrate formation. The pressure linearly decreases with the

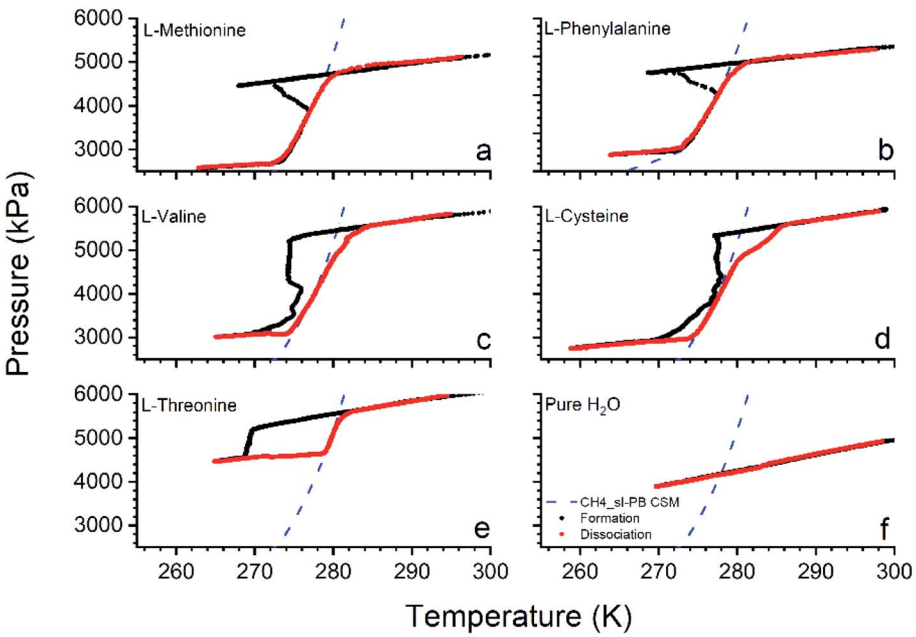

Fig. 2 Pressure–temperature profiles of methane hydrates formed in the presence of different amino acids. (a) l-Met, (b) l-phe, (c) l-val, (d) l-cys, (e) l-thr and (f) pure H_2O.

decrease in the temperature, and on heating/increasing the temperature, the gas linearly increases and retraces the cooling path. It shows that samples with no amino acids yield negligible hydrate formation, whereas those added with amino acids strongly influence methane hydrate occurrence. Methane gas forms structure I hydrate, and amino acids do not alter any structural properties.[49] It is evident from the hydrate dissociation pattern retracing the CH_4 sI phase equilibrium curve.[3]

3.2 CH_4 uptake and required subcooling for hydrate formation

This study's chosen amino acid powders have different hydrophobicity and functional groups. l-val, l-thr, l-cys, and l-met are compiled of aliphatic side chains, and l-phe is associated with an aromatic side-chain. l-Cys and l-met contain a sulfur atom in their side chain. l-val and l-thr also show some resemblance in the side chain configuration, namely, methyl group in l-val is replaced by a hydroxyl group in l-thr. As presented in Table 1, these amino acids show substantial variation in the degree of hydrophobicity. The highest (+4.2) is for l-val, and the least (−0.7 – hydrophilic) is for l-thr. Studies show that amino acids act as thermodynamic inhibitors. The hydrate inhibition is caused by perturbing the water structure by amino acids. The disruption of the hydrogen bond network by the amino acids delays hydrate formation. It clearly shows that the dissolution of the amino acids influences the physicochemical properties of hydrate formation.[37,38] Interestingly, some amino acids promote methane hydrate formation. The methane hydrate formation in the stirred tank reactor using L-histidine amino acid at 0.1 wt% and 1.0 wt% were studied. The observations showed improved kinetics compared to pure water. However, the overall gas uptake capacity is less than the 1 wt% sodium dodecyl sulfate.[50] In another study, the methane hydrates were tested in the presence of leucine amino acid, varying the amino acid concentration from 0.1 to 1.0 wt%. At 0.1 wt%, the system does not show any hydrate formation. Further increasing the concentration to 0.2 wt%, the methane hydrate formed, and the uptake capacity is about 137 mg g^{-1}. The maximum conversion is achieved when the amino acid concentration was 0.5 wt% with an uptake capacity of 143 mg g^{-1}, which is ∼94% of the maximum uptake capacity of 151 mg g^{-1} (hydration number 5.89), and the time taken for the 90% of the process conversion is nearly 20 minutes. With a further increase in the amino acid concentration to 1 wt%, there is a slight decrease in the uptake capacity (141 mg g^{-1}). The authors also investigated the methane hydrate formation with optimal 0.5 wt% amino acid in L-alanine, L-isoleucine, D-leucine, L-valine, and L-threonine. Out of five amino acids, L-isoleucine and D-leucine showed a higher conversion, nearly ∼143 mg g^{-1}. The maximum uptake capacity sightly decreased for L-valine and is about 138 mg g^{-1}. A significant decrement is seen for the L-threonine and is about 80 mg g^{-1}, which corresponds to ∼53% of the maximum uptake capacity. The L-alanine shows negligible hydrate conversion with no noticeable effect in hydrate promotion. It indicates that not all amino acids will promote/inhibit methane hydrate formation.[51] The methane hydrate morphology in the presence of leucine was studied. A methane bubble occurrence was observed at 0.3 wt% of leucine used during the hydrate growth. At concentrations above 0.3 wt%, mushy and indiscernible hydrate crystals were observed forming into the bulk solution. Once the methane bubble is triggered, the hydrate growth is observed at the gas–water interface. The hydrate crystals grow upward with the water supply through an increased capillary effect. The porous nature of forming hydrates with leucine amino acids enhances the gas–water interface, and higher hydrate conversion is achieved.[52]

The amount of subcooling required for the chosen amino acids in this study is shown in Fig. 3. The difference between the phase equilibrium temperature and the experimental formation temperature at the operating pressure is defined as subcooling. The amount of subcooling required for l-met and l-phe systems is about 8.05 ± 2 and 7.25 ± 2.1, and for l-val, it is about 5.4 ± 0.14. l-Cys system requires the least subcooling with an average value of 2.7 ± 0.8, and the highest subcooling is shown in the l-thr system with an average value of 10.75 ± 1.8. Since no formation is observed with the pure water system, we exclude it for comparison. The required subcooling with highest value in the increasing order is l-thr > l-met > l-phe > l-val > l-cys. The hydrophobicity is in the order l-val > l-phe > l-cys > l-met > l-thr. There is no relationship between hydrophobicity and hydrate inhibition. Several factors influence the hydrate promotion (i) the side chain molecular configuration and length (ii) amino acids interaction with water phase, (iii) hydrophobicity, solubility in water, (iv) density, viscosity, and refractive index.[53,54] It is difficult to ascertain the mechanism of the amino acids to one particular phenomenon.

The gas uptake capacity of the system defines the potential of methane hydrates as gas storage materials. The amount of gas captured with the chosen amino acids is shown in Fig. 4 and is calculated using eqn (1). The gas uptake capacity in l-met and l-phe is about 0.121 ± 0.008 and 0.123 ± 0.003 mol mol^{-1} H_2O, respectively. The l-val and the l-cys system are about 0.133 ± 0.004 and 0.138 ± 0.004 mol mol^{-1} H_2O, respectively. The

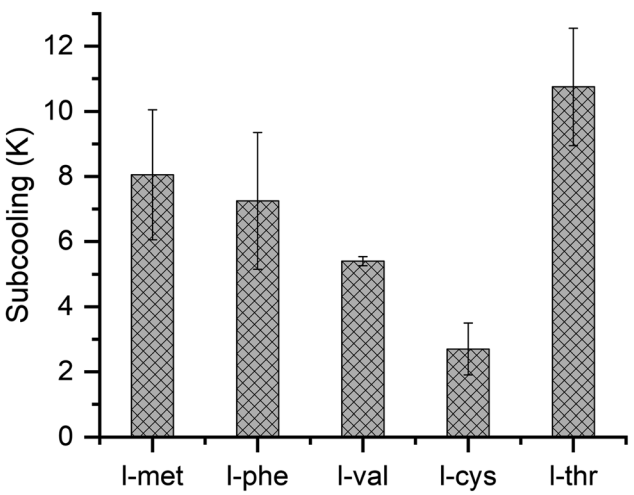

Fig. 3 Subcooling for methane hydrate formation in the presence of l-met, l-phe, l-val, l-cys, and l-thr amino acids.

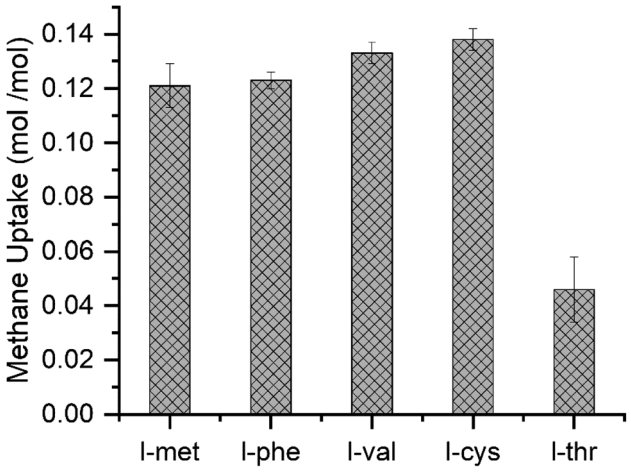

Fig. 4 The methane gas uptake capacity (mol mol^{-1}) in l-met, l-phe, l-val, l-cys, and l-thr amino acid systems.

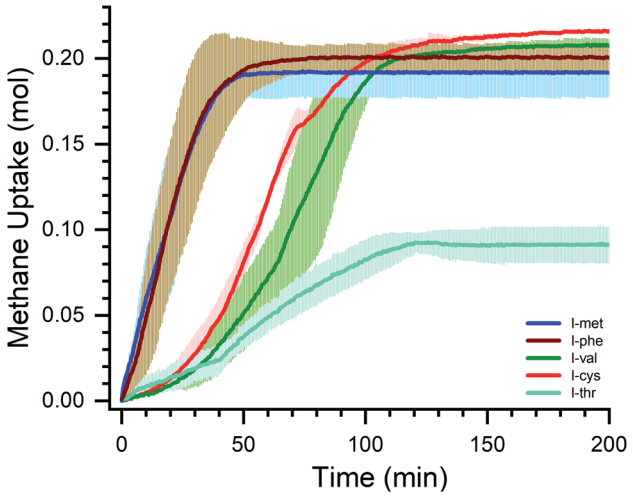

Fig. 5 Methane gas uptake kinetics in the presence of l-met, l-phe, l-val, l-cys, and l-thr amino acids.

lowest uptake capacity seen is l-thr which is about 0.046 ± 0.012 mol mol^{-1} H_2O which corresponds to ~29% of the maximum capacity of 0.158 mol mol^{-1} H_2O.[3] Similar uptake capacity is reported by Liu *et al.* with 0.5 wt% l-thr in the unstirred system. The total uptake was ~52% of the total uptake capacity.[51] The exact reason for this contrasting behavior of l-thr is obscure. The side chain of l-thr comprises the hydroxyl group, making it a polar and uncharged amino acid. Since hydroxyl groups alone can form hydrogen bonds with water, increasing the hydrophilicity and solubility of molecules containing them.[55] This phenomenon could be ascertained for lesser hydrate conversion. The other four amino acids, l-met, l-phe, l-val, and l-cys, show higher hydrate conversion, where l-cys is seen to be the highest with ~87% of the maximum uptake capacity.

3.3 CH_4 uptake kinetics

Another interesting factor in understating the role of additives is the gas uptake kinetics. The formation kinetics helps to understand the rate at which the reaction takes place and also to get insights into crystal formation. Fig. 5 shows the methane uptake kinetics in the presence of chosen amino acids. The full-time scale is shown up to 200 minutes where the hydrate saturation is achieved.

The methane uptake (mol) *vs.* time is shown in Fig. 5. The origin or the start point of kinetics is considered from the start of the hydrate nucleation. The kinetics of the five amino acids are shown in different color codes. The blue and brown lines represent the l-met and l-phe systems. The green and red lines represent the l-val and l-cys system, and the cyan represents the l-thr system. The data defined is the average of three repeat cycles (line), and a shaded portion is the standard deviation shown as an error. It is deceptive from the figure that the l-met and l-phe systems offer a high affinity for methane hydrates. The overall process is rapid and the t_{90} kinetics (time taken for completing 90% of the reaction) is within ~40 minutes. Though these systems' total gas uptake capacity is ~10% less than the l-cys system, the uptake kinetics are rapid.

The l-val and l-cys systems show sluggish kinetics for the first 30 minutes and slowly accelerate the process. The t_{90} kinetics is within ~102 minutes for these systems. The l-thr system shows delayed kinetics for the first 40 minutes, slowly picks up the process kinetics, and yields ~29% of the maximum hydrate conversion. The t_{90} kinetics is within ~100 minutes for this system. It is well known that the heat transfer coefficient will influence the process kinetics; it is ensured all the experiments are performed under similar conditions, and the heat transfer efficiency is the same. The hydrate growth process depends on several factors. Ideally, with no promoter and non-stirring, the methane hydrates do not nucleate at these operating conditions. Adding amino acids helps nucleate and accelerate the hydrate process in non-stirred conditions. Another critical parameter to study is the hydrate growth morphology.[52] In general, (no promoter) the hydrate nucleates at the gas–water interface and turns into a solid sheet blocking further gas to interact. In the presence of additives/promoters, the hydrate growth is observed to be downward or upward.[52] The concept of micellar theory and capillary theory influence these growth processes.[29] Ideally, if the hydrate growth triggers at the gas–water interface and the hydrates creep *via* capillary action and expose the hydrate surface to encase gas molecules, the kinetics would be faster and more rapid.[52,56] If the creep phenomenon is disrupted or the hydrate grows as a lump, it would be difficult for the gas to interact with the interstitial water.[56] The diffusion phenomenon limits the gas and water interaction. Also, the heat transfer within the hydrate is limited, which is responsible for weak hydrate growth and dawdling gas intake kinetics.[57,58]

The screened and selected amino acids show promising effects in the hydrate nucleation process. The overall gas uptake capacity is very high. It is observed that volume capacity (v/v) (calculated using eqn (2)) achieved is about 123.9 ± 1.1, 128.7 ± 6.4, 136.7 ± 3.1, 136.8 ± 3.1, and 50.4 ± 0.9 v/v for l-met, l-

phe, l-val, l-cys, and l-thr systems, respectively. All the amino acids show ~80–85% gas uptake capacity, whereas the l-thr is only about 30% of the achievable experimental limit (157.5 v/v). For real-time process development of methane hydrates for the gas capture and storage applications, the preferential order of amino acids based on the observed kinetics and uptake capacities is l-met ≪ l-phe ≪ l-cys ≪ l-val ≪ l-thr. Since these amino acids are readily soluble in water, they could be easily pelletized for methane gas storage and transportation.

4 Conclusions

To summarise, five commonly occurring amino acids were screened for methane gas storage in the form of hydrates. At operating pressure of 5500 kPa, the selected amino acids form hydrates around temperatures ~268 to 273 K except for l-cys, which is about ~277 K. The required subcooling for hydrates to trigger is high and is increasing in the order l-thr > l-met > l-phe > l-val > l-cys. The hydrate conversion is nearly high in all the amino acids with ~80–85% gas uptake capacity, except l-thr, which shows only 30% of the total uptake capacity. The gas uptake kinetics is faster in l-met and l-phe systems (t_{90} ~ 40 min), and sluggish kinetics is observed in l-cys, l-val, and l-thr systems. The preferential order of amino acids based on the observed kinetics and uptake capacities is l-met ≪ l-phe ≪ l-cys ≪ l-val ≪ l-thr. The investigation positively indicates using amino acids, l-met, l-phe, l-cys, and l-val as efficient materials for methane capture through the hydrate process.

Conflicts of interest

There are no conflicts to declare.

Acknowledgements

The authors sincerely thank the Director of CSIR-National Geophysical Research Institute, Hyderabad, for his encouragement and permission to publish this paper (NGRI/Lib/2022/Pub-21). Partial financial support from MoES (India) and DGH-NGHP (India) are acknowledged. The first author (BSK) acknowledges the Council of Scientific and Industrial Research (CSIR) for the Senior Research Fellowship (SRF-Direct).

References

1 *Importance of Methane*, https://www.epa.gov/gmi/importance-methane.
2 E. D. Sloan, *Natural gas hydrates in flow assurance*, Gulf Professional Publishing, 2010.
3 E. D. Sloan and C. A. Koh, *Clathrate hydrates of natural gases*, CRC press, 2007.
4 C. Sahu, R. Kumar and J. S. Sangwai, *Energy Fuels*, 2020, **34**, 11813–11839.
5 H. P. Veluswamy and N. Upadhye, *Energy Fuels*, 2022, **36**(5), 2323–2350.
6 Y. Zhu, P. Wang, S. Pang, S. Zhang and R. Xiao, *Energy Fuels*, 2021, **35**(11), 9137–9150.
7 W. F. Hao, J. Q. Wang, S. S. Fan and W. B. Hao, *Energy Convers. Manage.*, 2008, **49**, 2546–2553.
8 H. Kanda, *Economic Study on Natural Gas Transportation with Natural Gas Hydrate (NGH) Pellets*, Amsterdam, Netherlands, 2006.
9 S. K. Burla and S. R. P. Pinnelli, *Curr. Sci.*, 2022, **122**, 513–514.
10 M. Cha, K. Shin, J. Kim, D. Chang, Y. Seo, H. Lee and S. P. Kang, *Chem. Eng. Sci.*, 2013, **99**, 184–190.
11 A. Perrin, O. M. Musa and J. W. Steed, *Chem. Soc. Rev.*, 2013, **42**, 1996–2015.
12 A. Qasim, M. S. Khan, B. Lal, M. C. Ismail and K. Rostani, *Fuel*, 2020, **259**, 116219.
13 H. M. Stoner and C. A. Koh, *Fuel*, 2021, **304**, 121385.
14 S. Y. Misyura and I. G. Donskoy, *J. Nat. Gas Sci. Eng.*, 2022, **97**, 104324.
15 G. Bhattacharjee, H. P. Veluswamy, A. Kumar and P. Linga, *Chem. Eng. J.*, 2021, **415**, 128927.
16 C. A. Koh, E. D. Sloan, A. K. Sum and D. T. Wu, *Annu. Rev. Chem. Biomol. Eng.*, 2011, **2**, 237–257.
17 T. Uchida, B. Kvamme, R. Coffin, N. Tenma, A. Oyama and S. M. J. E. Masutani, *Energies*, 2017, **10**, 747.
18 Z. R. Chong, S. H. B. Yang, P. Babu, P. Linga and X.-S. Li, *Appl. Energy*, 2016, **162**, 1633–1652.
19 H. Dashti, L. Zhehao Yew and X. Lou, *J. Nat. Gas Sci. Eng.*, 2015, **23**, 195–207.
20 P. S. R. Prasad and C. V. V. Eswari, in *Carbon Utilization*, ed. M. Goel and M. Sudhakar, Springer, Singapore, 2017, ch. 11, pp. 157–168, DOI: DOI: 10.1007/978-981-10-3352-0_11.
21 P. Babu, A. Nambiar, T. He, I. A. Karimi, J. D. Lee, P. Englezos and P. Linga, *ACS Sustainable Chem. Eng.*, 2018, **6**, 8093–8107.
22 R. Liang, H. Xu, Y. Shen, S. Sun, J. Xu, S. Meng, Y. R. Shen and C. Tian, *Proc. Natl. Acad. Sci. U. S. A.*, 2019, **116**, 23410–23415.
23 W. Ke, T. M. Svartaas and D. Chen, *J. Nat. Gas Sci. Eng.*, 2019, **61**, 169–196.
24 S. N. Longinos and M. Parlaktuna, *Int. J. Chem. React. Eng.*, 2021, **19**, 155–165.
25 W. Ke and T. M. Svartaas, *Effects of stirring and cooling on methane hydrate formation in a high-pressure isochoric cell*, Edinburgh, United Kingdom, 2011.
26 S. N. Longinos and M. Parlaktuna, *ACS Omega*, 2021, **6**(2), 1636–1646.
27 S. N. Longinos and M. Parlaktuna, *React. Kinet., Mech. Catal.*, 2021, **132**, 771–794.
28 M. Tariq, M. R. C. Soromenho, L. P. N. Rebelo and J. M. S. S. Esperança, *Chem. Eng. Sci.*, 2022, **249**, 117319.
29 Y. He, M.-T. Sun, C. Chen, G.-D. Zhang, K. Chao, Y. Lin and F. Wang, *J. Mater. Chem. A*, 2019, **7**, 21634–21661.
30 P. S. R. Prasad, *J. Chem. Eng. Data*, 2015, **60**, 304–310.
31 B. Sai Kiran, K. Sowjanya, P. S. R. Prasad and J.-H. Yoon, *Oil Gas Sci. Technol.*, 2019, **74**, 12.
32 I. M. M. Vieira, B. L. P. Santos, D. S. Ruzene and D. P. Silva, *J. Ind. Eng. Chem.*, 2021, **100**(25), 1–18.
33 B. Kvamme, *Energy Fuels*, 2021, **35**, 17663–17684.
34 Y. Zeng, X. Niu, D. Lei, Z. Liu, Z. Zhu and W. Wang, *Sustainable Energy Fuels*, 2020, **4**, 4478–4481.

35 G. Bhattacharjee and P. Linga, *Energy Fuels*, 2021, **35**, 7553–7571.
36 J. Kyte and R. F. Doolittle, *J. Mol. Biol.*, 1982, **157**, 105–132.
37 J. H. Sa, G. H. Kwak, K. Han, D. Ahn, S. J. Cho, J. D. Lee and K. H. Lee, *Sci. Rep.*, 2016, **6**, 31582.
38 J.-H. Sa, G.-H. Kwak, K. Han, D. Ahn and K.-H. Lee, *Sci. Rep.*, 2015, **5**, 11526.
39 J. H. Sa, G. H. Kwak, B. R. Lee, D. Ahn and K. H. Lee, *Phys. Chem. Chem. Phys.*, 2014, **16**, 26730–26734.
40 J. H. Sa, G. H. Kwak, B. R. Lee, D. H. Park, K. Han and K. H. Lee, *Sci. Rep.*, 2013, **3**, 2428.
41 J. H. Sa, B. R. Lee, D. H. Park, K. Han, H. D. Chun and K. H. Lee, *Environ. Sci. Technol.*, 2011, **45**, 5885–5891.
42 C. B. Bavoh, B. Partoon, B. Lal, G. Gonfa, S. Foo Khor and A. M. Sharif, *Chem. Eng. Sci.*, 2017, **171**, 331–339.
43 H. Roosta, A. Dashti, S. H. Mazloumi and F. Varaminian, *J. Mol. Liq.*, 2016, **215**, 656–663.
44 P. S. R. Prasad and B. S. Kiran, *J. Nat. Gas Sci. Eng.*, 2018, **52**, 461–466.
45 K. Sowjanya and P. S. R. Prasad, *J. Nat. Gas Sci. Eng.*, 2016, **34**, 585–589.
46 Y. Sowjanya and P. S. R. Prasad, *J. Nat. Gas Sci. Eng.*, 2014, **18**, 58–63.
47 H. Khandelwal, M. F. Qureshi, J. Zheng, P. Venkataraman, T. A. Barckholtz, A. B. Mhadeshwar and P. Linga, *Energy Fuels*, 2020, **35**, 649–658.
48 B. S. Kiran and P. S. R. Prasad, *ACS Omega*, 2021, **6**, 8261–8270.
49 P. S. R. Prasad and B. Sai Kiran, *Sci. Rep.*, 2018, **8**, 8560.
50 G. Bhattacharjee, N. Choudhary, A. Kumar, S. Chakrabarty and R. Kumar, *J. Nat. Gas Sci. Eng.*, 2016, **35**, 1453–1462.
51 Y. Liu, B. Chen, Y. Chen, S. Zhang, W. Guo, Y. Cai, B. Tan and W. Wang, *Energy Technol.*, 2015, **3**, 815–819.
52 H. P. Veluswamy, Q. W. Hong and P. Linga, *Cryst. Growth Des.*, 2016, **16**, 5932–5945.
53 Q. Nasir, H. Suleman and Y. A. Elsheikh, *J. Nat. Gas Sci. Eng.*, 2020, **76**, 103211.
54 C. B. Bavoh, B. Lal, H. Osei, K. M. Sabil and H. Mukhtar, *J. Nat. Gas Sci. Eng.*, 2019, **64**, 52–71.
55 H. J. Cleaves, in *Encyclopedia of Astrobiology*, ed. M. Gargaud, R. Amils, J. C. Quintanilla, H. J. Cleaves, W. M. Irvine, D. L. Pinti and M. Viso, Springer Berlin Heidelberg, Berlin, Heidelberg, 2011, ch. 764, p. 793, DOI: 10.1007/978-3-642-11274-4_764.
56 S. K. Burla and S. R. P. Pinnelli, *RSC Adv.*, 2022, **12**, 2074–2082.
57 F. Rossi, M. Filipponi and B. Castellani, *Appl. Energy*, 2012, **99**, 167–172.
58 W. X. Pang, G. J. Chen, A. Dandekar, C. Y. Sun and C. L. Zhang, *Chem. Eng. Sci.*, 2007, **62**, 2198–2208.